Enhancement of ion generation in femtosecond ultraintense laser-foil interactions by defocusing

Xu, M. H.; Li, Y. T.; Carroll, D. C.; Foster, P. S.; Hawkes, S.; Kar, S.; Liu, F.; Markey, K.; McKenna, P.; Streeter, M. J. V.; Spindloe, C.; Sheng, Z. M.; Wahlström, Claes-Göran; Zepf, M.; Zheng, J.; Zhang, J.; Neely, D.

Published in:
Applied Physics Letters

DOI:
10.1063/1.3688027

2012

AIP | Applied Physics Letters

Enhancement of ion generation in femtosecond ultraintense laser-foil interactions by defocusing

M. H. Xu, Y. T. Li, D. C. Carroll, P. S. Foster, S. Hawkes et al.

Citation: Appl. Phys. Lett. **100**, 084101 (2012); doi: 10.1063/1.3688027
View online: http://dx.doi.org/10.1063/1.3688027
View Table of Contents: http://apl.aip.org/resource/1/APPLAB/v100/i8
Published by the American Institute of Physics.

Enhancement of ion generation in femtosecond ultraintense laser-foil interactions by defocusing

M. H. Xu,[1,2] Y. T. Li,[2,a)] D. C. Carroll,[3] P. S. Foster,[4] S. Hawkes,[4] S. Kar,[5] F. Liu,[2] K. Markey,[5] P. McKenna,[3] M. J. V. Streeter,[4] C. Spindloe,[4] Z. M. Sheng,[2,6] C.-G. Wahlström,[7] M. Zepf,[5] J. Zheng,[6] J. Zhang,[2,6] and D. Neely[4]

[1]*Department of Physics, China University of Mining & Technology (Beijing), Beijing 100083 China*
[2]*Beijing National Laboratory for Condensed Matter Physics, Institute of Physics, Chinese Academy of Sciences, Beijing 100080, China*
[3]*Department of Physics, SUPA, University of Strathclyde, Glasgow G4 0NG, United Kingdom*
[4]*Central Laser Facility, STFC, Rutherford Appleton Laboratory, Didcot, Oxon OX11 0QX, United Kingdom*
[5]*Centre for Plasma Physics, Queen's University Belfast, BT7 1NN, United Kingdom*
[6]*Department of Physics, Shanghai Jiao Tong University, Shanghai 200240, China*
[7]*Department of Physics, Lund University, P.O. Box 118, S-221 00 Lund, Sweden*

(Received 31 October 2011; accepted 1 February 2012; published online 21 February 2012)

A simple method to enhance ion generation with femtosecond ultraintense lasers is demonstrated experimentally by defocusing laser beams on target surface. When the laser is optimally defocused, we find that the population of medium and low energy protons from ultra-thin foils is increased significantly while the proton cutoff energy is almost unchanged. In this way, the total proton yield can be enhanced by more than 1 order, even though the peak laser intensity drops. The depression of the amplified spontaneous emission (ASE) effect and the population increase of moderate-energy electrons are believed to be the main reasons for the effective enhancement. © *2012 American Institute of Physics*. [doi:10.1063/1.3688027]

The generation of ion and proton beams in the ultraintense laser-plasma interactions has attracted much interest due to a variety of potential applications.[1–9] The target normal sheath acceleration (TNSA) mechanism[9] has been reported as an effective method to produce collimated ion beams with the current lasers. The proton acceleration is highly dependent on the contrast ratio of laser pulses.[10,11] For most intense laser systems currently used in the experiments, an ASE pedestal, which is typically 10^{-5} to 10^{-6} times the peak intensity, is presented before the main pulse. In this case, shock waves induced by the ASE pedestal will perturb the rear surface of the thin foils, resulting in the reduction of both the cutoff energy and the conversion efficiency of proton beams. Recent studies have indicated that utilizing high contrast laser pulses to irradiate ultra-thin foils is a promising way to improve the proton beam quality and conversion efficiency. Much effort has been made to improve the contrast ratio of the laser pulses, by utilizing the ultra-fast Pockels cells,[12] plasma mirrors,[13–15] second harmonic generation (SHG),[16] etc.

In this paper, we use a simple method to depress the ASE effect on the generation of proton beams. We experimentally show that the total yield and the cutoff energy (E_{cutoff}) from ultra-thin foils can be effectively enhanced by defocusing the laser beam for low contrast laser pulses (ASE pedestal of the order of 10^{-6} of the main pulse).

The experiment was performed with the Astra Ti-sapphire laser system at Rutherford Appleton Laboratory, which is capable of delivering up to 700 mJ energy in 50 fs at 10 Hz. The temporal contrast of the laser pulse was characterized by a third-order correlator, showing an ASE pedestal of the order 10^{-6} at 1 ns ahead. For some shots, a plasma mirror was introduced into the beam path, which increased the ASE contrast by 2 orders of magnitude (10^{-8}).[17] The p-polarized laser pulse was focused with an *f*/3 off-axis parabolic (OAP) mirror on aluminum foils at an incidence angle of 30°. The FWHM of the focal spot was measured to be around 5–6 μm when the laser was tightly focused. The targets used in the experiment were 50 nm and 2 μm Al foils.

The energy spectra of the proton beams were measured using two Thomson parabola spectrometers with a solid angle of 1.3×10^{-6} sr. One of them was aligned in the target normal direction and the other 8° away from the normal. The protons were recorded with a high-efficiency scintillator detector, which was optically coupled to an electron multiplying charge coupled device (EMCCD). In this case, real-time ion spectra over a range of 150 keV-6 MeV with an energy resolution of 100 keV at 1 MeV for protons were achieved. The spatial distributions of the proton beams were also measured with a real-time footprint image system, which consisted of a fast scintillator detector, optical imaging components and an intensified charge coupled device (ICCD) camera. The intensified gated camera was utilized to distinguish the proton signals from hot electrons and x rays with the time-of-flight method. Note only the lower half part of the proton beams was sampled [see Fig. 3(a)]. An electron magnetic spectrometer equipped with image plates was set in the laser propagation direction with a solid angle of 6.1×10^{-5} sr to measure the energy spectra of fast electrons. The defocusing scan was carried out by moving the OAP mirror. The peak laser intensity was reduced from 5×10^{19} W/cm^2 to the order of 10^{16} W/cm^2 by changing the offset from 0 (best focus position) to 500 μm, while the laser energy was kept as constant, with a shot to shot fluctuation less than 7%.

Figure 1 shows the energy spectra of the proton beams in the target normal direction when the laser is best focused

a)Electronic mail: ytli@aphy.iphy.ac.cn.

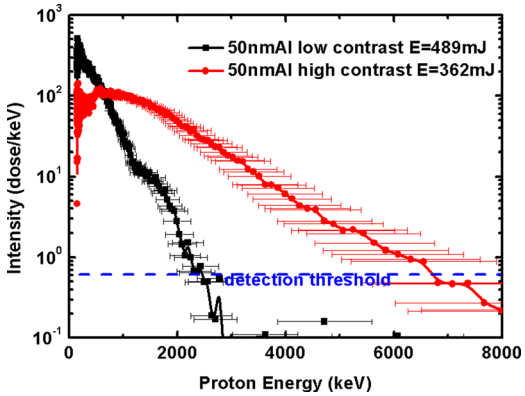

FIG. 1. (Color online) Energy spectra of proton beams with high contrast (10^{-8}) and low contrast (10^{-6}) laser pulses for the tight focus on 50 nm Al foils.

on a 50 nm aluminum foil. The E_{cutoff} for the high contrast shots (with plasma mirror) is about 6 MeV, while it is reduced to 2.4 MeV when no plasma mirror is utilized. Note that the laser energy for the low contrast shot is even larger than that for the high contrast. The spatial distributions of the proton beam generated from the 50 nm Al foils for different contrast laser pulses were also investigated. The results show similar depression of the proton flux when low contrast laser pulses are utilized.

Such a phenomenon can be understood by taking the ASE effect on the ion acceleration into account. For the low contrast laser beam, the intensity of the ASE pedestal is of an order of 10^{13} W/cm^2. This is high enough to create plasma at the front surface. In the case of the ultra-thin foils, the TNSA mechanism will become ineffective due to the preionization and the plasma expansion of the rear surface caused by the ASE pedestal.

In order to depress the ASE effect on the ion acceleration, we reduce the ASE intensity by defocusing the laser beam. The on-axis energy spectra of the proton beams emitted in the normal direction with various focal offsets are shown in Fig. 2(a). The cutoff energy is shown in Fig. 2(b). We find that the E_{cutoff} can be effectively increased by properly defocusing. When the laser is tightly focused, the E_{cutoff} is about 2.4 MeV. It reaches 3.5 MeV when the foil is 50 μm away from the best focal position. After that, the E_{cutoff} retained around 3 MeV even when the laser intensity is decreased substantially to 1.3×10^{17} W/cm^2 (300 μm offset). Finally, it rapidly drops down to 0.9 MeV when the offset is 500 μm. The maximum cutoff energy is achieved when the laser intensity is around 2.8×10^{18} W/cm^2 (50 μm offset). Similar phenomena are also observed by the off-axis Thomson spectrometer.

The energy spectra for 2 μm thick Al foils were also investigated. The E_{cutoff} for the 2 μm Al foil is also plotted in Fig. 2(b). When the laser is tightly focused, the E_{cutoff} for the 2 μm foil is around 6 MeV, which much exceed the E_{cutoff} for 50 nm foil. The reason is that when thicker foils are utilized, plasma formation at the rear surface induced by the ASE pedestal can be effectively suppressed, thus achieving a stronger acceleration field. Another feature revealed in Fig. 2(b) is that when the laser intensity gradually drops, a broad "plateau" region is presented between 2.7×10^{18} W/cm^2 and 1.7×10^{17} W/cm^2 for both targets, where the E_{cutoff} is retained around 3 MeV. The E_{cutoff} of 50 nm Al and 2 μm Al almost coincide with each other when the intensity is below 2.7×10^{18} W/cm^2.

We can also observe from Fig. 2(a) that when the focal offset increases, the population of the medium-energy and low-energy protons grows significantly. The population of the protons at 1 MeV $\pm$ 0.2 MeV [integrated over the shadowed range in Fig. 2(a)] with varied focal offsets is investigated and compared. It is found that for the 50 nm foil, the population of 1 MeV protons is enhanced by 90 times when the offset is 300 μm compared with that when the laser is tightly focused.

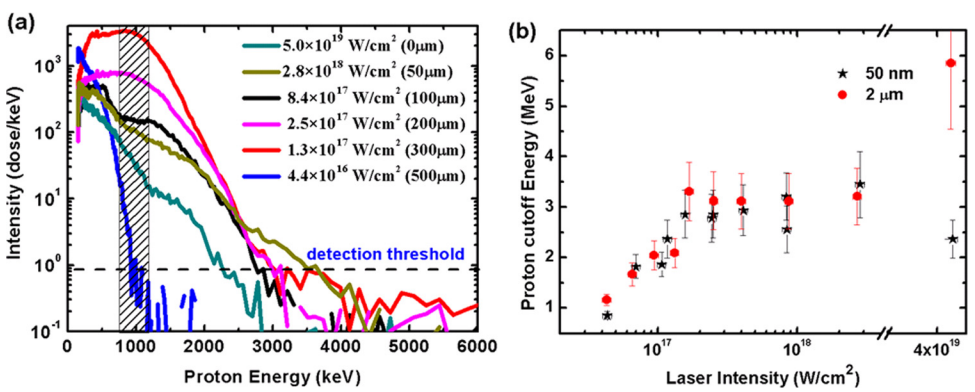

FIG. 2. (Color online) (a) Energy spectra of proton beams for 50 nm Al foils vs. laser intensities (focal offsets) for low contrast (10^{-6}) laser pulses. Laser energy is kept as constant. (b) The E_{cutoff} of proton beams vs. varied focal intensities for 50 nm (black star) and 2 μm (red dot) foils.

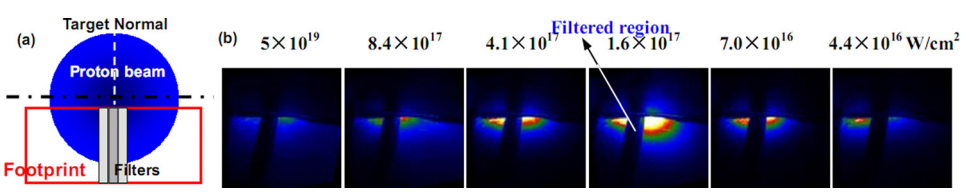

FIG. 3. (Color online) (a) Schematics of the ion beam footprint imaging system, which measures the spatial distribution of the lower part of the ion beam. The detector is covered by a set of filters with different thickness, which provides a rough energy resolution. (b) The spatial distributions of the proton beams from 50 nm foils for varied laser intensities. All the images are under the same color scale. The black gap shown in each image is due to the proton fluence reduction by the filters.

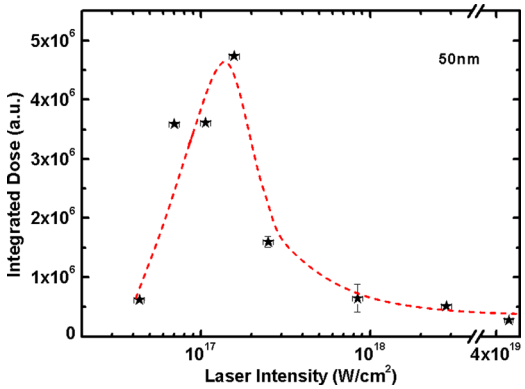

FIG. 4. (Color online) The proton dose of the whole beam under varied laser intensities.

The spatial distributions of the proton beams generated under varied focal offsets were also investigated using the real-time footprint imaging system sampling the lower part of the ion beam, as illustrated in Fig. 3. The spatial distributions also show obvious enhancement of proton emission by defocusing. The maximum enhancement of the protons with energy larger than 130 keV occurs at the laser intensity of 1.6×10^{17} W/cm^2.

The proton dose of the whole beam is estimated from the beam profiles and the energy spectra, see Fig. 4. We find that the dose increases significantly when the peak laser intensity drops. For the 50 nm Al, the proton dose can be enhanced 17 times by optimal defocusing of the laser beam. When the laser intensity is less than 1.6×10^{17} W/cm^2, the dose shows a rapid drop due to ineffective hot electron generation and therefore ineffective sheath acceleration. For the 2 μm aluminum, we find that the optimization of the proton dose is not as effective as that for the 50 nm foil. However, it can still be improved by 4-5 times compared to the tight focus case.

The significant enhancement of the proton beams by defocusing can be explained by taking two factors into account. The first one is the depression of the ASE effect on proton generation. When the laser beam is defocused, the intensity of the ASE pedestal will drop. The effect of the plasma expansion and the shock waves induced by the ASE on the proton acceleration is then effectively depressed, particularly in thin targets. In this way, the sheath field can be established more effectively than in the tight focus case, leading to more efficient acceleration.

The second factor is that when the laser beam is defocused, a larger population of fast electrons with moderate energy and low energy is generated because of the large focal area. Figure 5(a) shows the energy spectra of hot electrons in the forward direction when the laser intensity is reduced from 5×10^{19} W/cm^2 to 1.6×10^{17} W/cm^2 in the experiment. The graph shows that although the number of high energy electrons decreases when the laser intensity drops, the number of electrons with lower energy (less than 250 keV) increases. 2D particle-in-cell (PIC) simulations are also utilized to study the electron spectra under different focal offsets, which confirm the increase of population of moderate and low energy electrons as well. In the simulations, a p-polarized laser irradiates the target with an incidence angle of 25°. The normalized amplitude of the laser electric field at the focus is $a = a_0 \sin^2(\pi t/T)$, where a_0 is 2.0. The FWHM of the pulse is $10T_0$ and the duration is $24T_0$, where T_0 is the laser cycle. The thickness of the target is 2.5λ with a density of $4n_c$. A preplasma ranging from $x = 0$ to $x = 1\lambda$ with density distribution of $n = 0.54n_c\, e^{x/L}$ is presented before the target, in which L is 0.5λ. Figure 5(b) shows the energy spectra of electrons at $t = 30T_0$ when the focal offset is 0 (tight focus) and 27λ. It shows that when the target is 27λ away from the best focal position, the population of electrons with energy less than 500 keV is larger than that under the tight focus condition.

The number of protons accelerated from the rear surface can be approximately described by $N_p = \pi {d_L}^2 \lambda_D n_p$, where d_L is the transversal size of the sheath field, λ_D is the thickness of the sheath, and n_p is the density of protons being ionized. The large population of electrons for large focal spots can induce a sheath field over a large area on the rear surface. This may be one of the reasons for the intensity increase of medium-energy and low-energy protons in Fig. 2(c) and the broad "plateau" region in Fig. 2(b).

The role of the focal spot size plays in the proton acceleration process is not limited by just acting as a factor in determining the laser intensity. Brenner *et al.*[18] investigated the effect of the focal size separately using the high contrast Astra laser (to exclude the ASE effect). By comparing the datasets with the same laser intensity and different focal size, we can see that the maximum energy and the proton flux are closely related to the spot diameter. Another experiment carried on XL-II (Ref. 19) has found that the beam quality can be improved by defocusing the laser beam. Further investigations are needed to fully evaluate and understand the effect of spot size on the proton properties.

In conclusion, a simple method to enhance ion generation for low contrast (10^{-6}) lasers is demonstrated. The total

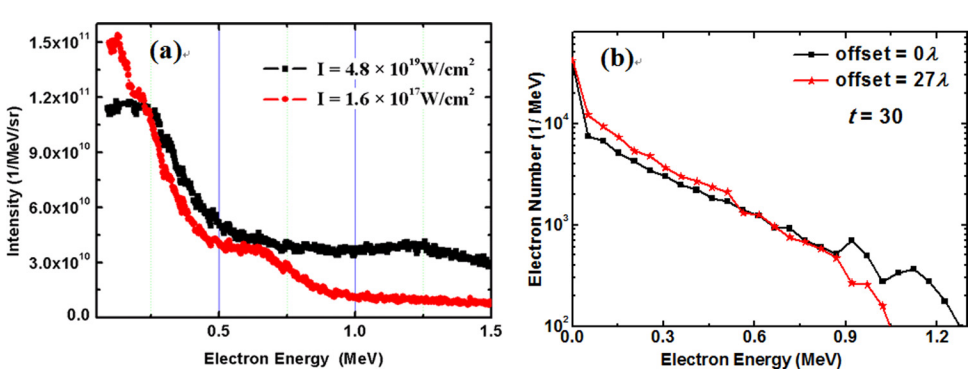

FIG. 5. (Color online) (a) Experimental energy spectra of hot electrons in the forward direction at the laser intensities of 4.8×10^{19} W/cm^2 (black line) and 1.6×10^{17} W/cm^2 (red line). (b) Simulated energy spectra of hot electrons when the target is at the best focal position (black square) and 27λ away from the best focal position (red star) at $t = 30T_0$.

yield and the cutoff energy of the proton beams from ultrathin foils can be effectively enhanced when the laser beams are optimally defocused. The depression of the influence of the ASE pedestal and the generation of large population of moderate-energy electrons are believed to be the main reasons for the enhancement.

This work was supported by the National Science Foundation of China (Grant Nos. 10925421, 10974250, 10935002), the Young Scientists Fund of the National Science Foundation of China (Grant No. 10905092), the National Basic Research Program of China (973 Programs) (Grant No. 2007CB815102), and the Fundamental Research Funds for the Central Universities. The authors would like to acknowledge Dr. Min Chen for useful discussions.

[1]B. M. Hegelich, B. J. Albright, J. Cobble, K. Flippo, S. Letzring, M. Paffett, H. Ruhl, J. Schreiber, R. K. Schulze, and J. C. Fernández, Nature **439**, 441 (2006).
[2]H. Schwoerer, S. Pfotenhauer, O. Jäckel, K.-U. Amthor, B. Liesfeld, W. Ziegler, R. Sauerbrey, K. W. D. Ledingham, and T. Esirkepov, Nature **439**, 445 (2006).
[3]D. Jung, L. Yin, B. J. Albright, D. C. Gautier, R. Hörlein, D. Kiefer, A. Henig, R. Johnson, S. Letzring, S. Palaniyappan *et al.*, Phys. Rev. Lett. **107**, 105002 (2011).
[4]M. Chen, A. Pukhov, T. P. Yu, and Z. M. Sheng, Phys. Rev. Lett. **103**, 24801 (2009).
[5]M. Roth, T. E. Cowan, M. H. Key, S. P. Hatchett, C. Brown, W. Fountain, J. Johnson, D. M. Pennington, R. A. Snavely, S. C. Wilks *et al.*, Phys. Rev. Lett. **86**, 436 (2001); N. Naumova, T. Schlegel, V. T. Tikhonchuk, C. Labaune, I. V. Sokolov, and G. Mourou, Phys. Rev. Lett. **102**, 025002 (2009).
[6]M. Borghesi, A. Bigongiari, S. Kar, A. Macchi, L. Romagnani, P. Audebert, J. Fuchs, T. Toncian, O. Willi, S. V. Bulanov *et al.*, Plasma Phys. Control. Fusion **50**, 124040 (2008).
[7]G. M. Dyer, A. C. Bernstein, B. I. Cho, J. Osterholz, W. Grigsby, A. Dalton, R. Shepherd, Y. Ping, H. Chen, K. Widmann *et al.*, Phys. Rev. Lett. **101**, 015002 (2008).
[8]E. Fourkal, I. Velchev, J. Fan, W. Luo, and C.-M. Ma, Med. Phys. **34**, 577 (2007).
[9]S. C. Wilks, A. B. Langdon, T. E. Cowan, M. Roth, M. S. Singh, S. P. Hatchett, M. H. Key, D. M. Pennington, A. J. Mackinnon, and R. A. Snavely, Phys. Plasmas **8**, 542 (2001).
[10]F. Lindau, O. Lundh, A. Persson, P. McKenna, K. Osvay, D. Batani, and C.-G. Wahlström, Phys. Rev. Lett. **95**, 175002 (2005); A. R. Holkundkar and N. K. Gupta, Phys. Plasmas **15**, 123104 (2008).
[11]M. H. Xu, Y. T. Li, X. H. Yuan, Q. Z. Yu, S. J. Wang, W. Zhao, X. L. Wen, G. C. Wang, C. Y. Jiao, Y. L. He *et al.*, Phys. Plasmas **13**, 104507 (2006).
[12]M. Kaluza, J. Schreiber, M. I. K. Santala, G. D. Tsakiris, K. Eidmann, J. Meyer-ter-Vehn, and K. J. Witte, Phys. Rev. Lett. **93**, 45003 (2004).
[13]D. Neely, P. Foster, A. Robinson, F. Lindau, O. Lundh, A. Persson, and C.-G. Wahlström, and P. McKenna, Appl. Phys. Lett. **89**, 21502 (2006).
[14]T. Ceccotti, A. Lévy, F. Réau, H. Popescu, P. Monot, E. Lefebvre, and Ph. Martin, Plasma Phys. Controlled Fusion **50**, 124006 (2008).
[15]T. Ceccotti, A. Lévy, H. Popescu, F. Réau, P. D'Oliveira, P. Monot, J. P. Geindre, E. Lefebvre, and Ph. Martin, Phys. Rev. Lett. **99**, 185002 (2007).
[16]L. M. Chen, M. Kando, M. H. Xu, Y. T. Li, J. Koga, M. Chen, H. Xu, X. H. Yuan, Q. L. Dong, Z. M. Sheng *et al.*, Phys. Rev. Lett. **100**, 45004 (2008).
[17]B. Dromey, S. Kar, M. Zepf, and P. Foster, Rev. Sci. Instrum. **75**, 645 (2004).
[18]C. M. Brenner, J. S. Green, A. P. L. Robinson, D. C. Carroll, B. Dromey, P. S. Foster, S. Kar, Y. T. Li, K. Markey, C. Spindloe *et al.*, Laser Part. Beams **29**, 345 (2011).
[19]M. H. Xu, Y. T. Li, F. Liu, Y. Zhang, X. X. Lin, F. Liu, S. J. Wang, L. M. Meng, Z. H. Wang, J. Zheng *et al.*, Acta Phys. Sin. **60**, 045204 (2011).